Analytical Methods

Cite this: *Anal. Methods*, 2012, **4**, 3169

www.rsc.org/methods

PAPER

Continuous-channel flow linear dichroism

Xi Cheng,[a] Maxim B. Joseph,[bc] James A. Covington,[c] Timothy R. Dafforn,[d] Matthew R. Hicks[ad] and Alison Rodger*[ae]

Received 21st May 2012, Accepted 15th August 2012
DOI: 10.1039/c2ay25513h

Linear dichroism (LD) is the difference in absorbance of light polarized parallel to a sample orientation axis and polarized perpendicular to it. Flow LD provides information about samples with high enough aspect ratios to be oriented in a flow stream. It is particularly useful for studying DNA–ligand systems, protein fibres and membrane assemblies and is the ideal technique for monitoring growth or destruction of particles. Standard Couette flow cells are limited to a dead time in kinetic processes of ~40 s (the assembly time). Recently an injection Couette flow cell has reduced the dead time to ~600 ms. In this paper we report an alternative system, based on syringe drives, 3 alternative flow-through cells, and the optical system of a Biologic MOS-450 spectrometer that has been adapted for LD. This system can reduce the dead time to 25 ms. The sample requirement is ~100 μL per time point. Less sample is required for longer dead times. The system has been applied to measure the kinetics of DNase digestion of DNA and GTP-induced polymerization of the bacterial cell division protein FtsZ.

Introduction

Linear dichroism (LD) is the difference in absorbance of light polarized parallel to a sample orientation direction and light polarized perpendicular to it. LD is non-zero only for samples that can be oriented. For samples oriented in shear flow, this means samples with a high aspect ratio (long and thin) in which case the orientation direction is the direction of the flow. Most flow LD data in the literature has been collected in Couette cell devices of various kinds.[1] Other flow orientation methods involve linear flow, either flow-through or oscillating flow as recently developed by Lundahl *et al.*[2]

Couette flow cell LD has proved useful to follow reactions involving the changes in orientation of chromophores on the timescale of minutes. Applications have included those where samples get longer or shorter, including polymerization and degradation of DNA; polymerization and depolymerization of fibrous proteins such as tubulin,[3] actin,[4,5] FtsZ,[6–8] and amyloid fibres;[4,9] and those where samples gain, lose or change orientation such as insertion of membrane peptides into membranes[10–13] or FtsZ bunding.[14] However, not all processes are as slow as these. We have recently developed an injection Couette flow cell that retains the advantages of Couette flow (recycling of the sample) while reducing the theoretical deadtime to 600 ms by introducing the sample *via* a hollow quartz rod in the centre of the cell.[15] This has enhanced our time window, but in practice this still misses the early stages of some kinetic processes in which we are interested, for example the formation of FtsZ protofilaments. Therefore, we have turned to technologies developed for stopped-flow to measure LD data.[16] As with stopped-flow experiments of any kind, the main disadvantage of this approach is the higher volume of sample required (in our case ~100 μL per time point) compared with the injection Couette cell approach (60–70 μL for a kinetic trace). However, in some cases the price is worth it.

In data analysis, the reduced LD (the LD divided by the isotropic absorbance) is often useful. It may be expressed as

$$\mathrm{LD}^{\mathrm{r}} = \frac{\mathrm{LD}}{A_{\mathrm{iso}}} = \frac{3}{2}\left(3\cos^2\theta_{\mathrm{s}} - 1\right)\left(3\cos^2\alpha - 1\right) \quad (1)$$

where α is the angle between the transition moment of interest and the long axis of the molecule and θ_{s} is the angle between the long axis of the molecule and the flow direction. In a sample we need to average over the $(3\cos^2\theta_{\mathrm{s}} - 1)$ term to account for a distribution of orientations, hence we may write

$$\mathrm{LD}^{\mathrm{r}} = \frac{3S}{2}\left(3\cos^2\alpha - 1\right) \quad (2)$$

The key challenges are to create a fast enough laminar flow to give a shear force that will orient the samples to be studied and a detection system to measure the LD signal. In this work we report a flow-through LD system based on a Biologic MOS-450 stopped flow instrument with three different types of flow-cell, illustrated in Fig. 1.

[a]*Department of Chemistry, University of Warwick, Coventry, CV4 7AL, UK. E-mail: a.rodger@warwick.ac.uk; Fax: +44 (0)24-76-575795; Tel: +44 (0)24-76574696*
[b]*MOAC Doctoral Training Centre, University of Warwick, Coventry, CV4 7AL, UK*
[c]*School of Engineering, University of Warwick, Coventry, CV4 7AL, UK*
[d]*Biosciences, University of Birmingham, Edgbaston, Birmingham, B15 2TT, UK*
[e]*Warwick Centre for Analytical Science, University of Warwick, Coventry, CV4 7AL, UK*

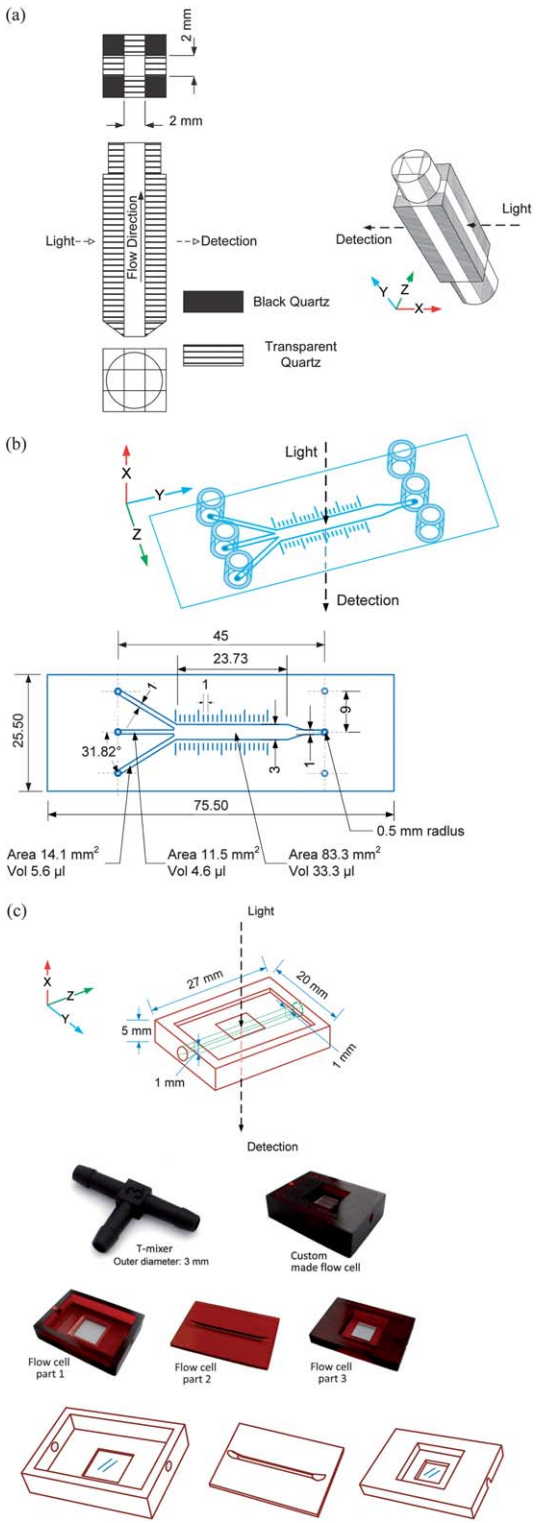

Fig. 1 Flow cells used in this work. Light is incident along *X*, *Z* is the parallel polarization of the light, which is not always the flow direction. (a) Quartz FC-20 cuvette that is inserted into the SFM-300 stopped-flow device. (b) The µ-slide III$^{3\ in\ 1}$ channel cell. (c) Custom-made single channel quartz window cell and the T-mixer used to mix input lines. The flow cell is assembled from three parts illustrated. All cells are oriented with respect to the light beam and the spectrometer-defined parallel polarization of the light which we define to be *Z*. Only for the Q1 × 1 cell does the flow direction align with *Z*.

(1) An FC-20 open cuvette with 2 mm × 2 mm square cross-section (which is supplied with the spectrometer by BioLogic) coupled to the Biologic SFM-300 unit to drive the solutions;

(2) A µ-slide III$^{3\ in\ 1}$ channel slide, coupled to a syringe pump to drive the solutions (denoted µ-Slide); and

(3) A custom-made 1 mm × 1 mm square cross-section flow cell with quartz windows coupled to a syringe pump to drive the solutions (denoted Q1 × 1).

Materials and methods

Materials

Highly lyophilized calf thymus DNA was obtained from Sigma and solutions were prepared by leaving DNA to hydrate in water overnight at 4 °C. FtsZ was prepared as described in ref. 17. All other chemicals were obtained from Sigma and used as received.

Continuous flow channel LD system

The three flow cells are shown in Fig. 1(a)–(c). The FC-20 was supplied by Biologic with the spectrometer. The µ-Slide III$^{3\ in\ 1}$ flow kit was purchased from ibidi (http://www.ibidi.de/products/disposables/S_8031X_SlideIII_3in1.html). We determined that 378 µL of water filled 18 cm of the tubing at room temperature. In our experiments, the spare inlet connections were blocked. The custom-made square cross-section Q1 × 1 flow cell was composed of three parts made by micro-stereolithography (MSL) and two pieces of optically clear quartz (Fig. 1(c)). In the MSL process a three dimensional object is made up by an additive layer manufacture technique where two dimensional cross-sections of an object are produced, layer after layer, until the final object is built. Each layer is made by photo cross-linking of the commercial R11 resin using a Perfactory Mini MuliLens system (Envisiontec, Gladbeck, Germany). Directly manufactured microfluidic flow cells made by this technique have been reported previously.[18,19] The parts were designed with a 50 µm tolerance to allow them to fit together. Two pieces of optically clear quartz were then sealed in place to allow optical access of the channel.

The SFM-300 system is usually used as a stopped-flow device, but because the stop is determined by when the drive syringes have delivered the required volume of liquid, it can be readily reconfigured to be a continuous-flow system. Two or three solutions can be mixed and injected into a sample cell. To perform continuous channel flow-LD, all the syringes of the SFM-300 unit were filled using a disposable plastic syringe containing 2 mL of sample or 2 mL of water. The SFM syringes were driven up and down several times to eliminate any bubbles and then the reservoir was filled. Alternatively, the syringe pump was used to deliver a fixed amount of sample at a fixed flow rate under the 'infuse only' mode. The LD signal at the selected wavelength was recorded under the transient recorder mode.

Couette flow LD

Couette flow LD spectra were collected with a Jasco J-815 circular dichroism spectropolarimeter adapted for LD equipped with a micro-volume Couette flow LD cell made by Crystal

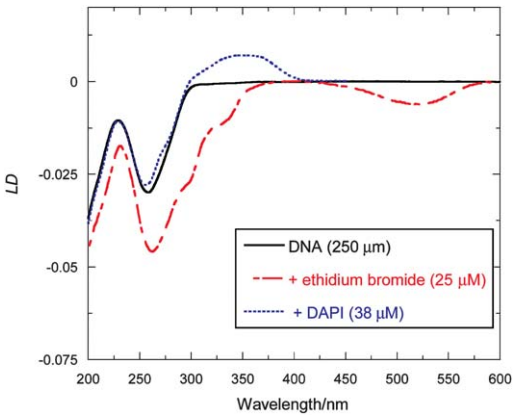

Fig. 2 Micro-volume capillary Couette flow cell LD spectrum of ct-DNA (250 mM) in water, with ethidium bromide (25 μM), and with 4′,6-diamidino-2-phenylindole (DAPI, 38 μM). Shear rate = 900 s^{-1}. (Spectra were collected in the course of work published in ref. 26 and 27.)

Precision Optics Rugby (now available from Kromatek, Great Dunmow, UK).

Results and discussion

Steady state LD of ct-DNA systems

In order to test the performance of the instrument and the different flow cells, LD spectra of well-known samples were collected. Calf thymus (ct) DNA was used for the two quartz cells and ct-DNA plus coloured ligands (ethidium bromide and DAPI) was used for the plastic μ-slide III$^{3\ in\ 1}$. B-DNA is a double helix whose spectroscopy over the wavelength ranges tested is due to π–π* transitions of the planar aromatic bases that lie approximately perpendicular (by convention at 86° (ref. 20)) to the helix axis.[21] The same is true of the intercalator ethidium bromide. By way of contrast, long-axis polarized transitions of minor groove bound ligands have a positive signal as illustrated by the DAPI 350 nm band. The Couette flow LD spectra for these systems are shown in Fig. 2. With the first two cells, the flow direction is perpendicular to the parallel direction of the light, so we expect to see signals of opposite sign from those illustrated.

LD of flowing systems

We first tested the magnitude of the signals that were obtained at different flow rates (and hence shear rates) for the different cells. Fig. 3 shows the LD signal of ct-DNA injected into the flow cells and Table 1 summarizes the flow parameters. Zero is the LD reading when there is no flow. In summary, lower shear rates have smaller LD signals and longer steady state measurements of the LD signal.

In the FC-20 cell, the DNA LD is positive (Fig. 3(a)) as the cell is oriented vertically so the flow direction aligns with the perpendicular polarization of the light. The flow rates in this cell are high and the corresponding sample consumption is high (see Table 1). After about 0.1 s of steady state LD signal, the signal decreases to zero due to the flow stopping. The slowest flow rate (1 mL s^{-1}) maintained the steady state LD signal the longest because it has the longest flow time. The maximum LD value was achieved by 2 mL s^{-1}. We suspect from the noise level that the flow is not laminar at 3 mL s^{-1}. Although the signal magnitudes are largest with this cell, the signal to noise is worst.

The μ-slide gave good quality data consistent with the Couette flow spectrum, of Fig. 2, from 300 nm upwards (the μ-slide was oriented so the flow direction aligns with the perpendicular polarization of the light giving −LD signals) as shown by the different wavelength measurements of Fig. 3(b). Data were also measurable over a wide range of shear rates (with the maximum of 310 s^{-1} being determined by the syringe pump). This system opens up the possibility of measuring reactions from 25 to 30 ms. The opposite signed LD signals observed for intercalated ethidium bromide/DNA solutions (Fig. 3(b) and (c)) and positive LD signals observed for DAPI/DNA solutions (LD = 0.0046 at 100 μL s^{-1} to LD = 0.0081 at 500 μL s^{-1}) show the variety of experiments that can be performed. The μ-Slide DNA LD signals

Table 1 Characteristics of the cells as used in our experiments. Shear rates were calculated according to ref. 24. Arrival time of samples can be varied by changing the length of the delay lines. The steady state LD signal was determined by averaging over the signals during the steady state phase. The dead times for each cell were determined by dividing the dead volume by the flow rate. The volumes are as follows: FC-20 cell from the SFM-300/400 User's Manual;[25] μ-slide and Q1 × 1 from the volume of the channel (Fig. 1, μ-slide main channel to measurement point is 17 μL; Q1 × 1 volume of tube between mixer to middle of the cell is 26 μL for the shortest line available)

Flow cell	Flow rate	Average shear rate	Duration of drive	Steady state LD signal	Dead-time	Volume per data point
FC-20 (2.5 mM DNA)	1 mL s^{-1}	620 s^{-1}	0.1446 s	0.020	76 ms (ref. 25)	239 μL
	1.5 mL s^{-1}	930 s^{-1}	0.12 s	0.026	51 ms	239 μL
	2 mL s^{-1}	1240 s^{-1}	0.0964 s	0.030	38 ms	239 μL
	2.5 mL s^{-1}	1553 s^{-1}	0.072 s	0.031	30 ms	239 μL
	3 mL s^{-1}	1863 s^{-1}	0.055 s	~0.033	25 ms	239 μL
μ-slide (250 μM DNA,	0.1 μL s^{-1}	0.06 s^{-1}	~1500 s	0.00025	270 s	150 μL
25 μM ethidium)	1 μL s^{-1}	0.6 s^{-1}	~150 s	0.001485	17 s	150 μL
	10 μL s^{-1}	6.2 s^{-1}	15 s	0.00437	1.7 s	150 μL
	100 μL s^{-1}	62 s^{-1}	1.51 s	0.00779	0.17 s	150 μL
	500 μL s^{-1}	310 s^{-1}	0.314 s	0.0108	0.034 s	150 μL
Q1 × 1 (250 μM DNA)	2 mL min^{-1}	166 s^{-1}	3.06 s	−0.015	0.78 s	100 μL
	3 mL min^{-1}	248 s^{-1}	2.09 s	−0.017	0.52 s	100 μL
	4 mL min^{-1}	332 s^{-1}	1.57 s	−0.019	0.39 s	100 μL
	5 mL min^{-1}	414 s^{-1}	1.24 s	−0.021	0.31 s	100 μL
	6 mL min^{-1}	496 s^{-1}	1.05 s	−0.022	0.26 s	100 μL

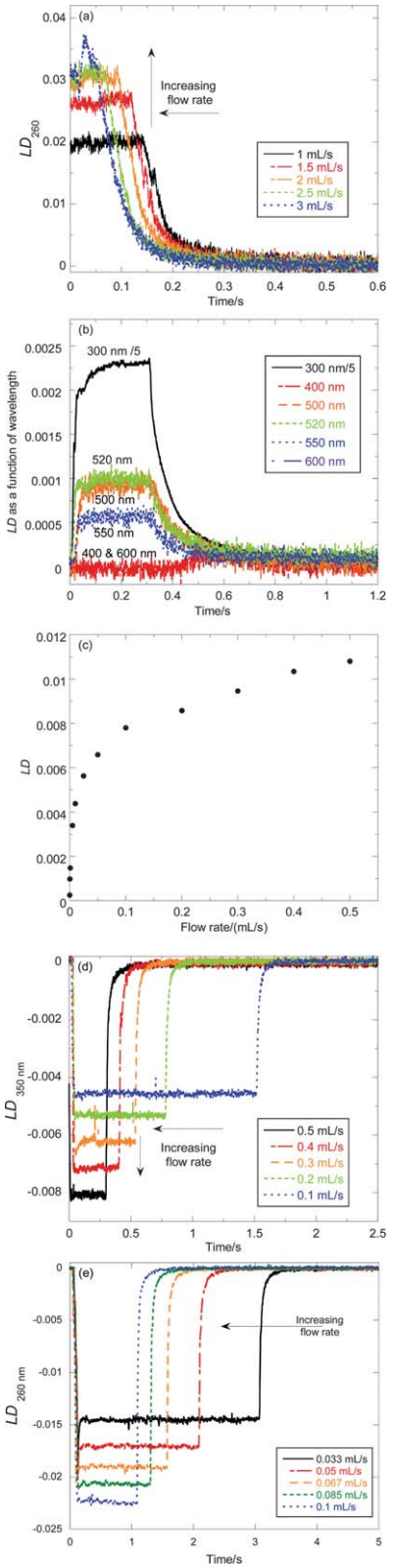

Fig. 3 (a) FC-20 cell LD measured at 260 nm as a function of time after the syringe drive was initiated for 239 μL ct-DNA (2.5 mM base); (b) μ-Slide LD for ct-DNA (250 μM) and ethidium bromide (25 μM) measured at different wavelengths. 150 μL of the solution was injected at 500 μL s^{-1} flow rate at each wavelength. (c) μ-Slide LD as for (b) but fixed wavelength (300 nm) and varying flow rate. (d) μ-Slide LD at 350 nm for ct-DNA (50 μM) and DAPI (7.5 μM). 150 μL of the solution was injected into at different flow rates. (e) Square cross-section quartz cell LD of ct-DNA (250 μM) at 260 nm as a function of flow rate. 100 μL of the solution was injected each time. Sampling period is 1 ms.

were linear with flow rate from 100 μL s^{-1} upwards. The sample consumed in this system is comparatively small. Its major drawback is the restriction to data collection above 300 nm.

The Q1 × 1 flow cell was augmented by a T-mixer to ensure sample mixing. We were able to orient this cell so that the flow direction was the parallel direction resulting in the more conventional negative LD signals for DNA (Fig. 3(e)). The Q1 × 1 cell shows much better behaviour and sample consumption than the FC-20. For example, an LD signal of 0.02 units required 2.5 mM ct-DNA flowed at 1 mL s^{-1} for FC-20 system, whereas the same magnitude was achieved for 250 μM ct-DNA at 0.083 mL s^{-1} in the Q1 × 1 cell. This is two orders of magnitude less sample to get better quality data. The DNA LD signals depended linearly upon flow rate in the 0.033 mL s^{-1} to 0.1 mL s^{-1} regime. We were concerned that part of the greater stability of this cell might be due poor mixing. We therefore compared the LD signals measured for 0.05 mL s^{-1} 250 μM DNA (LD = −0.009) and 0.025 mL s^{-1} DNA plus 0.025 mL s^{-1} water (*i.e.* the same net flow rate, LD = −0.017), and also 0.067 mL ms^{-1} DNA (LD = −0.010) and 0.033 mL s^{-1} DNA plus 0.033 mL s^{-1} water (LD = −0.019). The results are within 6% of what would be expected for a two-fold dilution in each case, though the discrepancy does suggest care is required in designing experiments involving mixing to ensure they are comparable. The deadtime of these measurements was of the order of 0.3 s.

Kinetics measurements

Although the μ-slide flow performance was the best, due to its limited wavelength range, we investigated the performance of the Q1 × 1 system to follow reaction kinetics. We varied the time of measurement by changing the length of the delay line from T-mixer to the detection point. The time point of a measurement was determined by initiating the solution injection and the data collection simultaneously. The time at which we detected the first LD signal after a flat baseline of approximately zero, was taken to be the time-point of the measurement. The data in Fig. 4 are for a relatively slow flow rate of 0.025 mL s^{-1} (the total flow rate was 0.05 mL s^{-1} due to two solutions being injected) to enable us to probe a reaction time course over a few seconds.

Fig. 4 shows data for the enzymatic hydrolysis of DNA by DNase I[15,22] into to smaller fragments that have a greatly reduced or no LD signal.[15] ct-DNA (250 μM) and DNase I (0.73 μM in 50 mM Tris–HCl, pH 8.0, 1 mM Ca_2Cl, 1 mM $MgSO_4$) were stored separately in two syringes. Nine different lengths of decay line were used with flow rates of 0.025 mL s^{-1} to monitor the time dependence of DNA digestion.

An analogous experiment (but with an additional time point using no connecting tube) was undertaken to probe the early stages of the polymerization of monomers of the protein FtsZ upon mixing with GTP (guanosine triphosphate) to form linear protofilaments. The backbone LD at 210 nm was used as the detection wavelength. Negative control experiments were also performed: when FtsZ and no GTP was injected into the flow cell

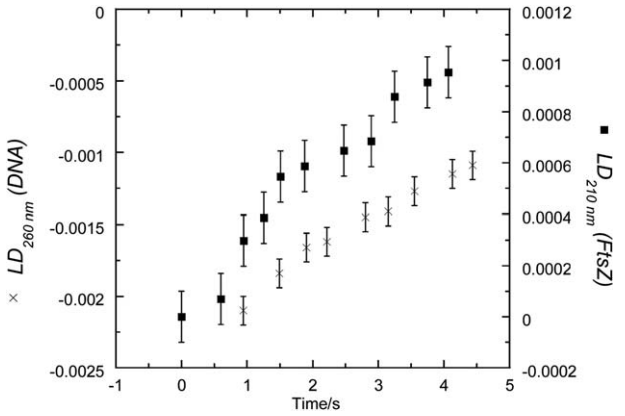

Fig. 4 LD as a function of arrival time in the detection window of ct-DNA(250 μM) and DNase I (0.73 μM) (left axis label) and $LD_{210\ nm}$ as a function of time after mixing of FtsZ (22 μM in100 mM MES–KOH, pH 6.5, 20 mM $MgCl_2$, 100 mM KCl) and GTP (0.4 mM). 300 μL of each solution was injected simultaneously at 1.5 mL min^{-1} for each delay line (making a total of 3 mL min^{-1}). Zero was defined to be the LD after the flow had ceased. Error bars are an estimate of the reproducibility of the data points.

no LD signal was observed. At first sight the early time data might be thought to be consistent with a lag phase in the polymerization kinetics. However, we have recently calculated the LD of FtsZ protofilaments of different lengths (to be published) which led us to predict that little LD signal would be observed until the protofilaments reached at least 7 subunits in length. Thus the apparent lag is a lag in LD detection rather than in polymerization. These data, combined with the calculations, thus have the potential to provide valuable input to understanding the mechanisms of complex reactions.

Conclusions

Here we have reported how LD signals can be measured for deadtimes as low as 25 ms. However, the cell that arguably provides the best balance between deadtime (33 ms) and sample consumption (150 μL), namely the μ-slide, is currently only available in plastic which precluded experiments using UV radiation. Work is in progress to design an adaptation to the μ-slide to have quartz windows. The 'home-made' Q1 × 1 quartz cell proved sufficient to monitor DNA digestion and FtsZ polymerization.

The time points for the kinetics applications explored herein were obtained by varying the length of the tubing between mixer and measurement point. This makes the experiment unnecessarily complicated. For the semi-rigid DNA systems we have shown that the LD magnitude depends linearly on flow rate above ~60 s^{-1}. It is also linearly dependent on concentration (as long as viscosity does not change much).[23] The dependence of LD signal on flow rate for rigid rods can be calculated according to ref. 24. This means that instead of varying the delay line, we could measure different time points by measuring data points as a function of flow rate and determining the percentage completion of a reaction as a function of time. The required scaling factors to determine LD as a function of time from LD as a function of shear rate require either initial or final LD signals (whichever is non-zero) as a function of shear rate. Two data points would be required. Alternatively a complete calibration curve could be measured. This approach would be somewhat more expensive in sample but simpler in terms of instrumentation as the delay line can be kept constant.

Acknowledgements

EPRSC is gratefully acknowledged for funding the MOAC Doctoral Training Centre and BBSRC for grant number BB/F011199/1.

Notes and references

1 B. Nordén, A. Rodger and T. R. Dafforn, *Linear Dichroism and Circular Dichroism: A Textbook on Polarized Spectroscopy*, Royal Society of Chemistry, Cambridge, 2010.
2 P. J. P. Johan Lundahl, C. C. Kitts and B. Nordén, *Analyst*, 2011, **136**, 3303–3306.
3 R. Marrington, M. Seymour and A. Rodger, *Chirality*, 2006, **18**, 680–690.
4 T. R. Dafforn, J. Rajendra, D. J. Halsall, L. C. Serpell and A. Rodger, *Biophys. J.*, 2004, **86**, 404–410.
5 D. Szczesna and S. S. Lehrer, *Biophys. J.*, 1992, **61**, 993–1000.
6 R. Marrington, E. Small, A. Rodger, T. R. Dafforn and S. G. Addinall, *J. Biol. Chem.*, 2004, **279**, 48821–48829.
7 R. Pacheco-Gomez, D. I. Roper, T. R. Dafforn and A. Rodger, *PLoS One*, 2011, **6**, e19369.
8 E. Small, R. Marrington, A. Rodger, D. J. Scott, K. Sloan, D. Roper, T. R. Dafforn and S. G. Addinall, *J. Mol. Biol.*, 2007, **369**, 210–221.
9 K. E. Marshall, M. R. Hicks, T. L. Williams, S. V. Hoffmann, A. Rodger, T. R. Dafforn and L. C. Serpell, *Biophys. J.*, 2010, **98**, 330–338.
10 A. Rodger, J. Rajendra, R. Marrington, M. Ardhammar, B. Norden, J. D. Hirst, A. T. B. Gilbert, T. R. Dafforn, D. J. Halsall, C. A. Woolhead, C. Robinson, T. J. Pinheiro, J. Kazlauskaite, M. Seymour, N. Perez and M. J. Hannon, *Phys. Chem. Chem. Phys.*, 2002, **4**, 4051–4057.
11 M. R. Hicks, T. R. Dafforn, A. Damianoglou, P. Wormell, A. Rodger and S. V. Hoffmann, *Analyst*, 2009, **134**, 1623–1628.
12 M. R. Hicks, A. Damianoglou, A. Rodger and T. R. Dafforn, *J. Mol. Biol.*, 2008, **383**, 358–366.
13 A. Damianoglou, A. Rodger, C. Pridmore, T. R. Dafforn, J. A. Mosely, J. M. Sanderson and M. R. Hicks, *Protein Pept. Lett.*, 2010, **17**, 1351–1362.
14 R. Marrington, E. Small, A. Rodger, T. R. Dafforn and S. Addinall, *J. Biol. Chem.*, 2004, **279**, 48821–48829.
15 M. R. Hicks, A. Rodger, Y.-P. Lin, N. C. Jones, S. V. Hoffmann and T. R. Dafforn, *Anal. Chem.*, 2012, **84**, 6561–6566.
16 D. Canet, K. Doering, C. M. Dobson and Y. Dupont, *Biophys. J.*, 2001, **80**, 1996–2003.
17 R. Pacheco-Gomez, D. I. Roper, T. R. Dafforn and A. Rodger, *PLoS One*, 2011, **6**(6), e19369, DOI: 10.1371/journal.pone.0019369.
18 R. D. Fisher, M. M. Mbogoro, M. E. Snowden, M. B. Joseph, J. A. Covington, P. R. Unwin and R. I. Walton, *ACS Appl. Mater. Interfaces*, 2011, **3**, 3528–3537.
19 M. E. Snowden, P. H. King, J. A. Covington, J. V. Macpherson and P. R. Unwin, *Anal. Chem.*, 2010, **82**, 3124–3131.
20 T. Matsuoka and B. Nordén, *Biopolymers*, 1982, **21**, 2433–2452.
21 A. Rodger, *Sci. Prog.*, 2008, **91**, 377–396.
22 C. N. N'soukpoé-Kossi, S. Diamantoglou and H. A. Tajmir-Riahia, *Biochem. Cell Biol.*, 2008, **86**, 244–250.
23 E. L. Gilroy, M. R. Hicks, D. J. Smith and A. Rodger, *Analyst*, 2011, **136**, 4159–4163.
24 J. McLachlan, D. J. Smith, N. P. Chmel and A. Rodger, *Soft Matter*, 2012, submitted.
25 Biologic, *SFM-300/400 User's Manual. Ver. 2.1*, 2005.
26 C. Dicko, M. R. Hicks, T. R. Dafforn, F. Vollrath, A. Rodger and S. V. Hoffmann, *Biophys. J.*, 2008, **95**, 5974–5977.
27 R. Marrington, T. R. Dafforn, D. J. Halsall and A. Rodger, *Biophys. J.*, 2004, **87**, 2002–2012.